

## METAL-PHOSPHONATE CHEMISTRY: SYNTHESIS, CRYSTAL STRUCTURE OF CALCIUM-AMINO- TRIS-(METHYLENE PHOSPHONATE) AND INHIBITION OF $\text{CaCO}_3$ CRYSTAL GROWTH

Konstantinos D. Demadis and Stella D. Katarachia  
Department of Chemistry, University of Crete,  
Heraklion, Crete, Greece

(Received May 6, 2003; accepted December 2, 2003)

*Organic (poly)phosphonates are additives in water treatment that find broad use as mineral scale and corrosion inhibitors for a plethora of industrial applications. The phenomenon of precipitation of scale inhibitors has been studied intensively. This study reports the synthesis, characterization, and crystal structure of a Ca salt of AMP (AMP = Amino-tris-Methylene Phosphonate). Ca-AMP crystals are monoclinic, space group  $P 2_1/n$  with unit cell dimensions,  $a = 11.3382(5) \text{ \AA}$ ,  $b = 8.4555(4) \text{ \AA}$ ,  $c = 15.5254(7) \text{ \AA}$ ,  $\beta = 90.6551^\circ$ ,  $V = 1488.33(12) \text{ \AA}^3$  and  $Z = 4$ . The structure is polymeric due to chelation of multiple Ca ions by AMP. The  $\text{Ca}^{2+}$  center is slightly distorted octahedral and is surrounded by five phosphonate oxygens and a water molecule.  $\text{Ca}-\text{O}(\text{P})$  bond lengths range from 2.2924(14) to 2.3356(14)  $\text{ \AA}$ . The  $\text{Ca}-\text{O}(\text{H}_2\text{O})$  bond distance is 2.3693(17). Each phosphonate group is monodeprotonated, and the nitrogen atom is protonated.  $\text{CaCO}_3$  inhibition and crystal modification by AMP are also reported, together with synergistic effects with polyacrylate-based terpolymers.*

**Keywords:** AMP; calcium carbonate; dispersant polymers; phosphonate; scale formation; scale inhibition

Industrial water systems face several challenges related to formation of sparingly soluble electrolytes.<sup>1</sup> Cooling water systems, in particular, may suffer from a multitude of problems, including fouling, corrosion, and biofilm growth. Utility plants, manufacturing facilities, refineries,

The authors wish to acknowledge Dr. Peter White for collecting the X-ray data and Nalco Chemical Company for supplying samples of polymers A and B.

Address correspondence to Konstantinos D. Demadis, Department of Chemistry, University of Crete, Heraklion GR-71409, Crete, Greece. E-mail: demadis@chemistry.uoc.gr

air-conditioning systems, just to mention a few, use “hot” processes in their operations. These have to be cooled. Water is a universal cooling medium because of its cost-effectiveness and its high heat capacity.<sup>2</sup> After cooling water comes in contact with the “hot” process, it needs to be re-cooled for reuse. Cooling is achieved by partial water evaporation. The end result is concentration of all species found in the water until a critical point of “scaling,” leading to precipitation, and ultimately deposition of mineral salts. Species usually associated with these deposits (depending on water chemistry) are calcium carbonate, calcium phosphate(s), silica/metal silicates *etc.* Such undesirable deposition issues can be avoided with careful application of chemical water treatment techniques.<sup>3</sup>

Prevention of scale formation is greatly preferred by industrial water users to the more costly (and often potentially hazardous) alternative of chemical cleaning<sup>4</sup> of the adhered scale, in the aftermath of a scaling event. Silica and silicate salts are classic examples of scales that require laborious (mechanical) and potentially dangerous (hydrofluoric acid) cleaning.<sup>5</sup> Prevention of scale deposition can also benefit the water operator by eliminating (or at least by minimizing) unexpected production shut-downs and by offering substantial savings through water conservation (especially in arid areas with high water costs).

Organophosphorous compounds, usually referred to as organic phosphates or phosphonates, are an integral part of a water treatment program.<sup>6</sup> They function as scale inhibitors by adsorbing onto crystal surfaces of insoluble salts, thus preventing further crystal growth.<sup>7</sup> At high  $\text{Ca}^{2+}$  levels phosphonates can precipitate out of solution as  $\text{Ca}^{2+}$  salts. Unfortunately, this is a very common problem in cooling water systems.<sup>8</sup> Such precipitates can be detrimental to the entire cooling water treatment program because:

- (a) They cause depletion of soluble inhibitor, and, subsequently, poor scale control because inhibitor unavailability in solution to inhibit scale formation.
- (b) They can act as potential nucleation sites for other scales.
- (c) They can deposit onto heat transfer surfaces (they are known to have inverse solubility characteristics) and cause poor heat flux, much like other known scales, such as calcium carbonate, calcium phosphate, *etc.*).
- (d) If corrosion inhibition is the purpose of the phosphonate inhibitor, its precipitation as a  $\text{Ca}^{2+}$  salt will eventually lead to poor corrosion control.

In other applications, such as oilfield drilling,<sup>9</sup> precipitation of scale inhibitors as  $\text{Ca}^{2+}$ ,  $\text{Ba}^{2+}$ , or  $\text{Sr}^{2+}$  salts is desirable. Large amounts

of inhibitor are “squeezed” in the oilfield well and remain there for a specified amount of time, during which the inhibitor precipitates with alkaline earth metals found in high-salinity brine. Eventually it deposits onto the rock formation. Once the well is opened again for operation the metal-inhibitor salts slowly dissolve to provide adequate levels of scale inhibitor in solution.<sup>9</sup> Controlled dissolution of these salts is essential, as fast dissolution will lead to chemical wastage and slower dissolution will result in inefficient scale control. Knowledge of the chemistry of Ca-phosphonate salts under varying conditions of temperature and ionic strength can provide valuable information. Wise and effective use of such knowledge can lead to the discovery of new and better performing scale inhibitors. Schematic structures of some extensively used, “traditional” scale inhibitors are shown in Figure 1.

Phosphonates usually contain multiple phosphonate groups ( $\text{R-PO}_3\text{H}_2$ , R = organic chain) most commonly found in their deprotonated form, due to the particular pH range of operation (virtually all open recirculating cooling water systems operate at pH's in the range 7.0 to 9.8). These additives perform scale inhibition in ppm quantities and usually work synergistically with dispersant polymers. Aminomethylene phosphonates in particular are used extensively in cooling water treatment programs,<sup>10</sup> oilfield applications<sup>9</sup> and corrosion control.<sup>11</sup> AMP is one of the most common aminomethylene phosphonates and a very effective scale inhibitor.<sup>12</sup> However, under certain conditions (high  $\text{Ca}^{2+}$  concentrations, high pH) it forms Ca-AMP precipitates, which have the detrimental effects mentioned above. Some patented technologies based on polymers have been reported to effectively control Ca-AMP scale.<sup>13</sup>

Understanding the intimate mechanisms of scale inhibition by phosphonates requires a closer look at the molecular level of their possible function. The present study aims towards this direction. In this report, the preparation, characterization, and crystal structure of a Ca-AMP complex salt are reported. In addition, results on the properties of AMP as a  $\text{CaCO}_3$  scale inhibitor and a surface modifier together with its synergistic function with dispersant polymers are reported as well.

## EXPERIMENTAL SECTION

Deionized water was used for all experiments. Materials were obtained from commercial sources. AMP (in acid form, 50% in water) was obtained from Solutia UK, Newport, United Kingdom,  $\text{CaCl}_2 \cdot 2\text{H}_2\text{O}$  was from Fischer Scientific, and CaO was from Aldrich Chemical Co, Milwaukee, WI, U.S.A. Polymers A and B were proprietary products from

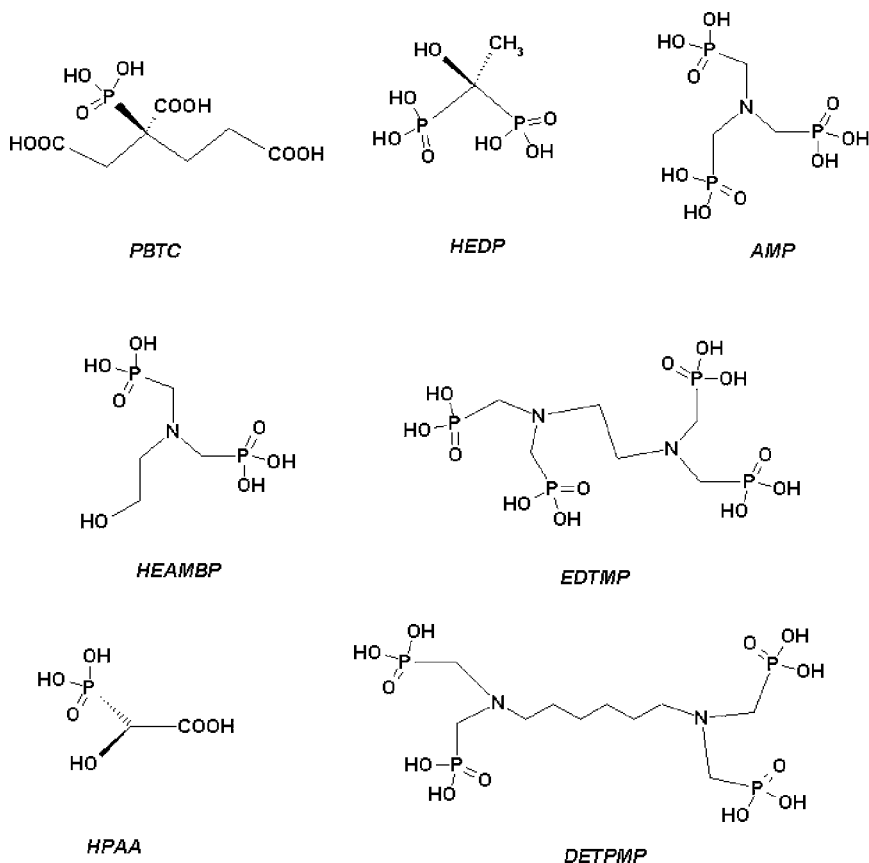


**FIGURE 1** Schematic structures of some widely used scale inhibitors in their acid forms. The symbol abbreviations are as follows: PBTC 2-phosphonobutane-1,2,4-tricarboxylic acid, HEDP 1-hydroxyethylidene-1,1-diphosphonic acid, AMP amino-*tris*-(methylenephosphonic acid), HEAMP 2-hydroxyethyl-amino-*bis*-(methylenephosphonic acid), EDTMP ethylene-diamine-*tetrakis*-(methylene-phosphonic acid), HPAA hydroxy-phosphonoacetic acid, DETPMP hexamethylene-diamine-*tetrakis*-(methylene-phosphonic acid).

Nalco Chemical Company, Naperville IL, U.S.A. Polymers A and B are acrylate/acrylamide/alkylsulfonate terpolymers with different degree of sulfonate groups. A has higher number of acrylate and lower degree of sulfonate groups than B and both have molecular weights of  $\sim 18,000$  daltons.<sup>14</sup>

## Preparation of Ca-AMP Complex Salt

### *From AMP and $\text{CaCl}_2 \cdot 2\text{H}_2\text{O}$*

An amount AMP (5.0 mL of a 0.5 M stock solution in DI water) was acidified with 10% HCl until the pH was 1.5. Subsequently, an amount of a solution of  $\text{CaCl}_2 \cdot 2\text{H}_2\text{O}$  (5.0 mL, 0.5 M in DI water) was added under vigorous stirring, while the pH was constantly monitored. The pH dropped and was re-adjusted to 1.5 by addition of 0.1 N NaOH solution. The beaker was covered and set aside. During a crystallization process of about 24 h, large ( $0.25 \times 0.20 \times 0.10$  mm), transparent crystals of the title compound (rectangular plates) formed and were isolated by filtration. They were washed with deionized water and air-dried. Elemental Analysis was done on a sample dried at 105°C. Calculated for  $\text{CaC}_3\text{H}_{12}\text{P}_3\text{O}_{10}\text{N}$  (MW 355.18): C, 10.1; H, 3.4; N, 3.9; Ca, 11.3. Measured: C, 10.0; H, 3.4; N, 3.7; Ca, 10.7.

### *From AMP and CaO*

A quantity of CaO (5.0 g, 89.3 mmol) was suspended in 50 mL deionized water causing the pH to go to 12. A 50% AMP solution (40 mL, 1:1 molar ratio) was added dropwise and CaO started dissolving as the pH decreased to 1.5. A white precipitate formed immediately. It was filtered and air-dried. Yield 26 g (70%). Elemental Analysis was done on a sample dried at 105°C. Calculated for  $\text{CaC}_3\text{H}_{12}\text{P}_3\text{O}_{10}\text{N}$  (MW 355.18): C, 10.1; H, 3.4; N, 3.9; Ca, 11.2. Measured: C, 10.0; H, 3.3; N, 3.7; Ca, 10.0.

## X-Ray Structure Determination: Data Collection, Solution and Refinement of the Structure

Single crystals suitable for crystallographic determination were obtained by reacting AMP and CaO, by using 1/5 of the above quantities. Several regularly shaped (rectangular plates), colorless crystals were selected, sealed in an air-tight vial (to avoid water loss) for single crystal X-ray data collection. Relevant information concerning crystal data, intensity collection information, and structure refinement parameters for the structure are provided in Table I. Data were collected at  $-100^\circ\text{C}$  using a cold stream of evaporated liquid  $\text{N}_2$  to minimize thermal motion. Standard crystallographic methods (direct methods) were used to initially locate the heavier atoms in the structure. The remaining non-hydrogen atoms were located in subsequent difference Fourier maps. Empirical absorption corrections were applied with SADABS. The ORTEP plotting program was used to computer-generate

**TABLE I** Summary of Crystal Data, Intensity Collection and Structure Refinement Parameters for [Ca(AMP)(H<sub>2</sub>O)]·3.5H<sub>2</sub>O

Salt	Ca[N(CH <sub>2</sub> PO <sub>3</sub> H) <sub>3</sub> ]·3.5H <sub>2</sub> O
Formula	CaC <sub>3</sub> H <sub>19</sub> P <sub>3</sub> O <sub>13.50</sub> N
Molecular weight	418.18
a (Å)	11.3382(5)
b (Å)	8.4555(4)
c (Å)	15.5254(7)
α(deg)	90
β(deg)	90.655(1)
γ(deg)	90
V (Å <sup>3</sup> )	1488.33(12)
Z	4
Crystal system	Monoclinic
Space group	P 2 <sub>1</sub> /n
Crystal size (mm)	0.25 × 0.20 × 0.10
d <sub>calcd</sub> (g/cm <sup>3</sup> )	1.866
Diffractometer	Siemens CCD Smart
Radiation	Mo Kα (λ = 0.71073 Å)
Collection temperature	−100°C
Absorption coefficient μ, cm <sup>−1</sup>	0.81
F(000)	870.78
2θ <sub>max</sub> (deg)	60.0
Total reflections	19990
Unique reflections	4283
Refined reflections (I <sub>net</sub> > 2.5σI <sub>net</sub> )	3441
Merging R value	0.025
Number of parameters	199
R (%) <sup>a</sup> (R (%), all reflections)	2.9(3.6)
R <sub>w</sub> (%) <sup>b</sup> (R <sub>w</sub> (%), all reflections)	3.9(4.0)
Goodness of fit <sup>c</sup>	1.54
Deepest hole (e/Å <sup>3</sup> )	−0.570
Highest peak (e/Å <sup>3</sup> )	0.660

$$^a R = \Sigma(|F_o - F_c|) / \Sigma|F_o|.$$

$$^b R_w = [\Sigma(w|F_o - F_c|)^2 / \Sigma w(F_o)^2]^{1/2}.$$

$$^c \text{GoF} = [\Sigma w(F_o - F_c)^2 / (\text{no. of reflections} - \text{no. of parameters})]^{1/2}$$

the structural views shown in Figures 2, 3, 4 and 5.<sup>15</sup> All atoms were refined anisotropically. Hydrogen atoms were located in the difference Fourier map and refined as well. All computations were performed by using the NRCVAX suite of programs.<sup>16</sup> Atomic scattering factors were taken from a standard source<sup>17</sup> and corrected for anomalous dispersion.

The crystal of Ca-AMP contains 3<sup>1</sup>/<sub>2</sub> H<sub>2</sub>O molecules *per* asymmetric unit. Final positional parameters, along with their standard deviations as estimates from the inverse matrix are given in Table II. Selected bond distances and angles in Ca-AMP are given in are given in Table III.

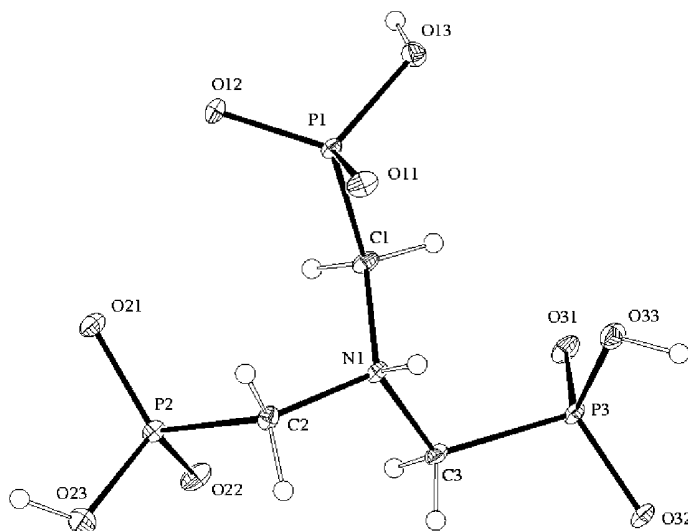


**FIGURE 2** ORTEP diagram of the AMP portion of the structure. Ca atoms are not shown in this view. Protonated phosphonate and amine nitrogen groups can be clearly seen.

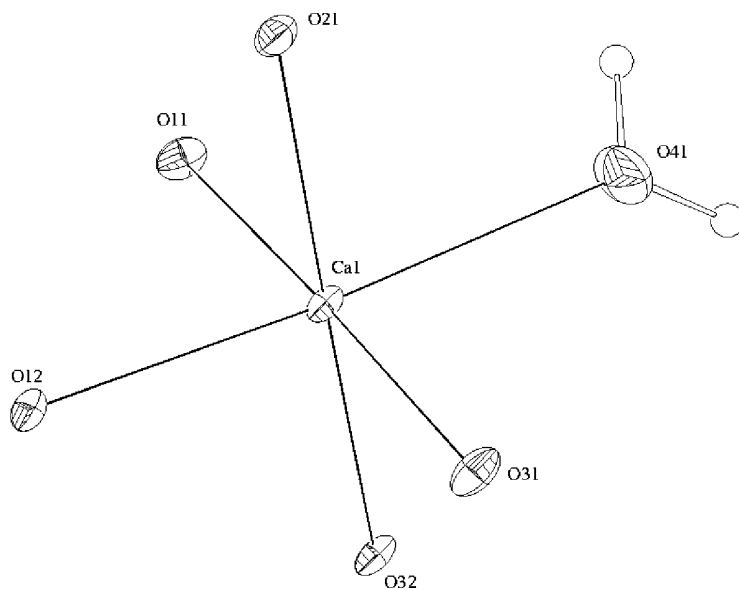


**FIGURE 3** Octahedral coordination environment of Ca. O(12) and O(21) are from the same AMP molecule that acts as a bidentate chelate. O(41) is the coordinated water. O(11), O(31) and O(32) come from three different, monodentate AMP ligands.

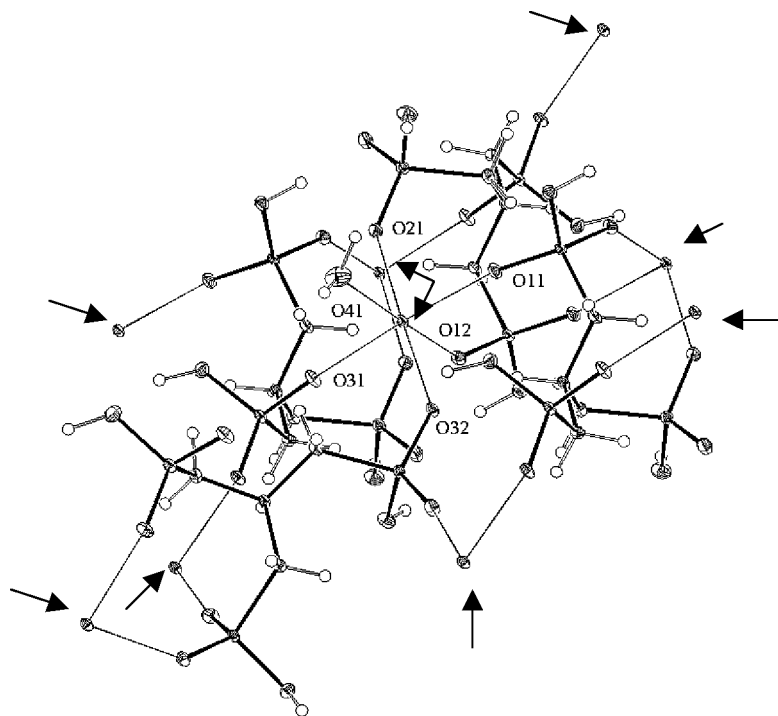


**FIGURE 4** Coordination environment of the Ca center and next neighboring Ca atoms. Ca atoms are indicated by arrows.

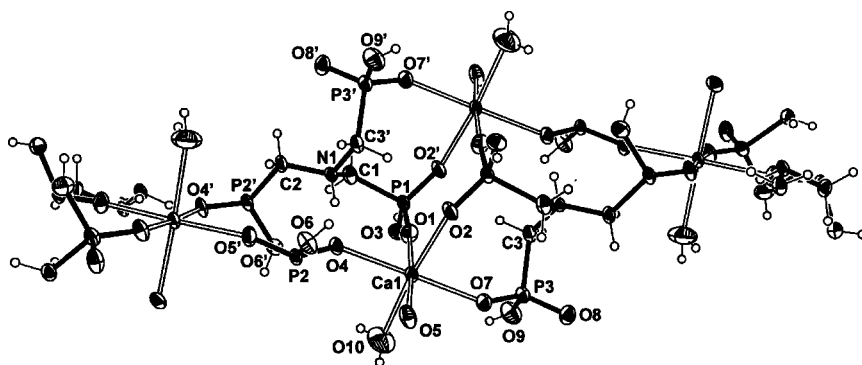


**FIGURE 5** Another view of the structure of Ca-AMP showing part of the polymeric structure. Numbering scheme is different from that in Figure 4.



**TABLE II** Atomic Parameters x, y, z and  $B_{\text{iso}}$  for  $[\text{Ca}(\text{AMP})(\text{H}_2\text{O})] \cdot 3.5\text{H}_2\text{O}$ . Estimated Standard Deviations (esd's) Refer to the Last Digit Printed

Atom	x	y	z	$B_{\text{iso}}$
Ca1	0.96216(3)	0.65621(4)	0.162759(24)	0.855(13)
P1	1.07916(4)	0.27872(6)	0.06649(3)	0.819(16)
P2	1.23683(5)	0.79883(6)	0.07356(3)	1.017(18)
P3	0.80290(5)	1.01366(6)	0.24295(3)	0.861(17)
N1	0.84123(14)	0.22070(19)	0.10379(10)	0.85(6)
C1	0.95612(18)	0.14117(23)	0.08373(13)	1.07(7)
C2	1.21182(18)	0.69128(23)	-0.02765(12)	1.02(6)
C3	0.75301(17)	1.10877(24)	0.14289(12)	1.01(6)
O11	1.04605(12)	0.43273(17)	0.10658(9)	1.33(5)
O12	0.88746(12)	0.72220(17)	0.02695(8)	1.20(5)
O13	1.18358(12)	0.20529(17)	0.12164(9)	1.21(5)
O21	1.12640(12)	0.80309(17)	0.12627(9)	1.27(5)
O22	1.28864(13)	0.95863(17)	0.05470(10)	1.52(5)
O23	1.33432(14)	0.69222(20)	0.11669(10)	1.82(6)
O31	0.86739(13)	0.86513(17)	0.22108(9)	1.42(5)
O32	0.80407(12)	0.49460(16)	0.20091(9)	1.07(5)
O33	0.89199(13)	1.13737(18)	0.28155(9)	1.44(5)
O41	1.05239(16)	0.61315(23)	0.29915(11)	2.75(7)
O42	0.5187(3)	0.9814(4)	0.04443(20)	2.05(13)
O43	0.85651(15)	0.2279(3)	0.43740(11)	2.83(8)
O44	0.49076(18)	0.37464(24)	0.08090(13)	3.45(8)
O45	0.27421(17)	0.46328(21)	0.22547(11)	2.76(7)

<sup>a</sup> $B_{\text{iso}}$  is the Mean of the Principal Axes of the Thermal Ellipsoid.

Tables of hydrogen atom parameters, anisotropic thermal parameters, and observed/calculated structure amplitudes are available from the author.

## Calcium Carbonate Scale Inhibition Test

$\text{Ca}^{2+}$ ,  $\text{Mg}^{2+}$ , and  $\text{HCO}_3^-$  are expressed as ppm  $\text{CaCO}_3$ , whereas AMP and polymeric additives as ppm actives. Stock solutions of 40,000 ppm of  $\text{CaCl}_2 \cdot 2\text{H}_2\text{O}$ ,  $\text{NaHCO}_3$  and  $\text{MgSO}_4 \cdot 7\text{H}_2\text{O}$  were prepared using de-ionized water. Appropriate amounts of stock solutions were used to achieve final concentrations of  $\text{Ca}^{2+}$ ,  $\text{Mg}^{2+}$ , and  $\text{HCO}_3^-$ . In a volumetric flask  $\text{Ca}^{2+}$ ,  $\text{Mg}^{2+}$  were mixed and then the appropriate amount of inhibitor was added. Finally, the desired amount of  $\text{NaHCO}_3$  was added and the remaining volume was made up with de-ionized water. Depending on the test analysis requirements, the final volume of the test solution was between 100–500 mL. The solution was then transferred to an Erlenmeyer flask. The flask was covered and placed in a water

**TABLE III** Selected Bond Distances (Å), Angles (Deg) and Torsion Angles (Deg) in [Ca(AMP)(H<sub>2</sub>O)]·3.5H<sub>2</sub>O

Bond distances					Bond angles				
Ca(1)—O(11)	2.2924(14)				O(11)—Ca(1)—O(12)	90.07(5)			
Ca(1)—O(12)	2.3309(14)				O(11)—Ca(1)—O(21)	90.61(5)			
Ca(1)—O(21)	2.3142(15)				O(11)—Ca(1)—O(31)	175.60(5)			
Ca(1)—O(31)	2.2622(14)				O(11)—Ca(1)—O(32)	86.40(5)			
Ca(1)—O(32)	2.3356(14)				O(11)—Ca(1)—O(41)	92.10(6)			
Ca(1)—O(41)	2.3693(17)				O(12)—Ca(1)—O(21)	86.29(5)			
P(1)—C(1)	1.8382(20)				O(12)—Ca(1)—O(31)	90.33(5)			
P(1)—O(11)	1.4931(15)				O(12)—Ca(1)—O(32)	95.59(5)			
P(1)—O(12) a	1.5036(14)				O(12)—Ca(1)—O(41)	173.68(6)			
P(1)—O(13)	1.5802(14)				O(21)—Ca(1)—O(31)	93.79(5)			
P(2)—C(2)	1.8347(20)				O(21)—Ca(1)—O(32)	176.47(5)			
P(2)—O(21)	1.5040(15)				O(21)—Ca(1)—O(41)	87.75(6)			
P(2)—O(22)	1.5034(15)				O(31)—Ca(1)—O(32)	89.20(5)			
P(2)—O(23)	1.5703(16)				O(31)—Ca(1)—O(41)	87.96(6)			
P(3)—C(3)	1.8330(20)				O(32)—Ca(1)—O(41)	90.47(6)			
P(3)—O(31)	1.4942(15)				C(1)—P(1)—O(11)	107.24(8)			
P(3)—O(32) b	1.5102(14)				C(1)—P(1)—O(12) a	109.69(9)			
P(3)—O(33)	1.5684(15)				C(1)—P(1)—O(13)	103.75(9)			
N(1)—C(1)	1.5019(25)				O(11)—P(1)—O(12) a	118.29(9)			
N(1)—C(2) a	1.5155(25)				O(11)—P(1)—O(13)	107.89(8)			
N(1)—C(3) c	1.5094(25)				O(12) a—P(1)—O(13)	109.00(8)			
O(32)—P(3) e	1.5102(14)				C(2)—P(2)—O(21)	110.88(9)			
					C(2)—P(2)—O(22)	109.61(9)			
					C(2)—P(2)—O(23)	100.47(9)			
					O(21)—P(2)—O(22)	114.46(9)			
					O(21)—P(2)—O(23)	111.59(8)			
					O(22)—P(2)—O(23)	108.92(9)			
					C(3)—P(3)—O(31)	108.86(9)			
Torsion angles									
O12	Ca1	O11	P1	−62.88(11)	O21	Ca1	O11	P1	−149.17(17)
O31	Ca1	O11	P1	32.33(9)	O32	Ca1	O11	P1	32.72(9)
O41	Ca1	O11	P1	123.06(16)	O11	Ca1	O21	P2	13.35(8)
O12	Ca1	O21	P2	−76.68(12)	O31	Ca1	O21	P2	−166.76(17)
O32	Ca1	O21	P2	45.58(10)	O41	Ca1	O21	P2	105.43(15)
O11	Ca1	O31	P3	−111.78(15)	O12	Ca1	O31	P3	−16.58(8)
O21	Ca1	O31	P3	69.72(12)	O32	Ca1	O31	P3	−112.17(15)
O41	Ca1	O31	P3	157.33(18)	O11	P1	C1	N1	19.69(15)
O13	P1	C1	N1	133.7(3)	C1	P1	O11	Ca1	−29.04(11)
O13	P1	O11	Ca1	−140.24(17)	C2	P2	O21	Ca1	35.72(12)
O22	P2	O21	Ca1	160.34(19)	O23	P2	O21	Ca1	−75.39(14)
C3	P3	O31	Ca1	8.28(11)	O33	P3	O31	Ca1	−103.41(16)

bath maintained at 43°C. The solution inside the flask was under constant stirring with a magnetic stirring bar. pH 8.8 was maintained by addition 0.1 N NaOH *via* an auto-titrator. After a time period of 2 h the flask was removed from the water bath and a sample was filtered through a 0.45  $\mu$  filter. Analysis by atomic absorption spectroscopy gave the concentration of soluble  $\text{Ca}^{2+}$ . The remaining solution was covered and stored *unstirred* at room temperature. A second set of samples was withdrawn from just below the surface 24 h after the pH was first raised to 8.8. The analytical results of these *unfiltered* samples yielded the dispersed  $\text{Ca}^{2+}$  concentration.

## RESULTS AND DISCUSSION

### Preparation of Calcium-AMP Complex Salt

AMP has seven dissociable phosphonate protons, if the N–H proton is taken into account. At pH 1.5 one to two protons can dissociate from AMP.<sup>9f</sup> However, in presence of high  $\text{Ca}^{2+}$  levels (or a metal ion in general) acidity enhancement of the remaining protons occurs. In the case of the Ca-AMP salt described herein, three phosphonate protons dissociate resulting in an overall charge of “2-” on the AMP ligand. A Ca-AMP precipitate was reported by Fogler et al. that appears to be very similar to the one described here.<sup>9f</sup> It has a Ca:AMP molar ratio of 1:1 and crystallizes in the form of platelets that seem to have their edges rounded. By comparison, the Ca-AMP crystalline precipitate herein also crystallizes in rectangular plates with well-defined edges.

### Crystal Structure and Lattice

The complexity of the polymeric structure can be seen in Figures 4 and 5. There are no discrete molecular units of the Ca-AMP complex. Instead, the methylenephosphonate “arms” participate in an intricate network of *intermolecular* and *intramolecular* interactions involving  $\text{Ca}^{2+}$  centers and hydrogen bonds. The result is a complex polymeric three-dimensional structure caused mainly by multiple bridging of the AMP molecules. Each phosphonate group is monodeprotonated. The protonated O atom (–P–O–H) remains non-coordinated. The remaining two P–O groups bridge two neighboring Ca atoms in a Ca–O–P–O–Ca arrangement.

There are four Ca-AMP “units” per unit cell. The overall Ca:AMP molar ratio is 1:1. Electroneutrality is achieved by charge balance between the divalent Ca and the triply deprotonated/monoprotonated AMP

ligand. There are also  $3\frac{1}{2}$  water molecules in the unit cell. One is coordinated to Ca. Water molecules of crystallization serve as "space fillers" and also participate in extensive hydrogen bonding superstructures.

## COORDINATION ENVIRONMENT OF THE $\text{Ca}^{2+}$ CENTER

The intimate coordination environment of the Ca atom is shown in Figure 3. The Ca is surrounded by six oxygens, five from phosphonate groups and one from water. Ca—O(P) distances range from 2.2924(14) to 2.3356(14) Å. The Ca—O(H<sub>2</sub>O) distance is 2.3693(17) Å, somewhat longer than Ca—O(P) distances. The Ca atom is situated in a slightly distorted octahedral environment, as judged by the O—Ca—O angles, which show slight deviations from idealized octahedral geometry (see Table III). Ca—O(P) bond lengths can be compared to similar bonds found in the literature (*vide infra*).

One AMP ligand *per* Ca acts as a bidentate chelate, forming an eight-member ring. Each  $\text{Ca}^{2+}$  center is coordinated by four AMP phosphonate oxygens in a monodentate fashion. Each of these methylenephosphonate groups is simultaneously coordinated to a neighboring Ca atom. A water molecule completes the octahedron.

## PHOSPHONATE GROUPS

All three phosphonate groups in AMP are mono-deprotonated. This formally separates the P—O bonds into three groups: P—O—H (protonated), P=O (phosphoryl), and P—O<sup>−</sup> (deprotonated). The P—O(H) bond lengths are 1.5684(15) Å, 1.5703(16) Å, and 1.5802(14) Å. On the other hand, P=O and P—O<sup>−</sup> bond lengths are crystallographically indistinguishable and are found in the 1.4931(15)–1.5102(14) Å range. This observation coupled with the fact that all Ca—O(P) distances are very similar, point to the conclusion that the negative charge on each  $-\text{PO}_3\text{H}^-$  is delocalized over the O—P—O moiety. It is worth-noting that only the deprotonated P—O groups coordinate to the Ca atoms, whereas the protonated P—OH's remain non-coordinated. P—C bond lengths are unexceptional, 1.8382(20) Å, 1.8347(20) Å and 1.8330(20) Å.

## ENVIRONMENT OF THE NITROGEN ATOM

N—C bond lengths are 1.5019(25), 1.5155(25) Å, and 1.5094(25) Å. The C—N—C angles are  $\sim 112^\circ$ . The N is protonated (the H atom was located in the difference Fourier map and refined).

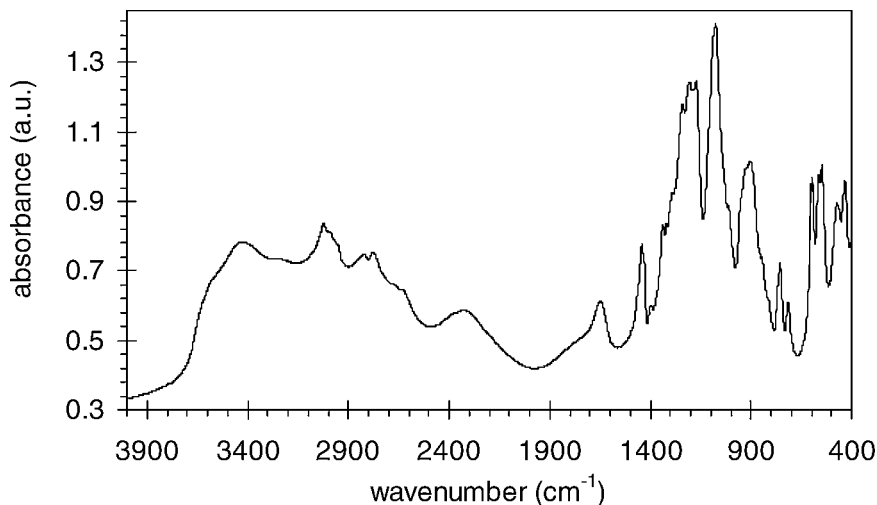


**FIGURE 6** FT-IR spectrum of Ca-AMP in KBr pellets.

### Vibrational Characterization and Analysis<sup>18</sup>

An FT-IR spectrum of Ca-AMP (Figure 6) displays a multitude of bands. Band assignments are given in Table IV. Bands in the region 1180–1240  $\text{cm}^{-1}$  are assigned to the P=O stretch. The characteristic P–OH band appears at 2350  $\text{cm}^{-1}$ . A medium intensity band at 1661  $\text{cm}^{-1}$  is assigned to the –P(O)(OH) group. The N–H stretch from the protonated amino group appears as a shoulder at 2700  $\text{cm}^{-1}$ .  $\text{Me}_3\text{NH}^+$  shows its N–H stretch in a similar position. A strong band at 1080  $\text{cm}^{-1}$  is due to the C–N stretching vibration, whereas the C–N deformation appears at 1342  $\text{cm}^{-1}$ . A weak band at 758  $\text{cm}^{-1}$  is tentatively assigned to the P–C stretch. O–H stretches from water appear as broad bands at 3450 and 3260  $\text{cm}^{-1}$ . The –CH<sub>2</sub>– symmetric and antisymmetric stretches give rise to a group of bands in the 3030–2790  $\text{cm}^{-1}$  region. Deformation of –CH<sub>2</sub>– appears at 1440  $\text{cm}^{-1}$ .

### Calcium Phosphonate Structural Chemistry

Crystal and molecular structures of *mono*-phosphinates<sup>19</sup> and *mono*-phosphonates<sup>20</sup> have been extensively studied. Also, an extensive number of *bis*-phosphonate<sup>21</sup> structures exist, but only a limited number of  $\text{Ca}^{2+}$ -*bis*-phosphonate structures have been reported.<sup>22</sup> Furthermore,

**TABLE IV** Infrared Band Assignments for  $[\text{Ca}(\text{AMP})(\text{H}_2\text{O})]\cdot 2.5\text{H}_2\text{O}^a$ 

Band ( $\text{cm}^{-1}$ )	Assignments
3450 (m), 3260 (m)	$\nu_3 + \nu_1$ stretches of H-bonded $\text{H}_2\text{O}$
3030 (m), 3022 (m), 3015 (m), 3000 (m)	$\text{CH}_2$ antisymmetric stretch
2850 (m), 2790 (m)	$\text{CH}_2$ symmetric stretch
2700 (sh)	$\text{N}-\text{H}^+$ stretch
2350 (w, br)	$\text{P}-\text{OH}$ stretch
1660 (m)	$\nu_2$ bend of H-bonded $\text{H}_2\text{O}$
1440 (m)	$\text{CH}_2$ deformation
1400 (w)	$\text{CH}_2$ bend
1342 (m)	$\text{C}-\text{N}$ deformation
1320 (m), 1290 (m)	$\text{CH}_2$ wag or twist
1240 (s), 1210 (s), 1181 (s)	$\text{PO}_3$ antisymmetric stretch
1080 (vs)	$\text{C}-\text{N}$ stretch
1020 (sh)	?
908 (m)	$\text{P}-\text{O}$ stretch
850 (w)	$\text{CH}_2$ rock
758 (w)	$\text{P}-\text{C}$ stretch
719 (w)	$\text{H}_2\text{O}$ libration
592 (m)	$\text{PO}_3$ bend
567 (m), 548 (m)	$\text{PO}_3$ bend

<sup>a</sup>s, strong; m, medium; w, weak; sh, shoulder.

*ab initio* studies on relevant organophosphorous compounds and their Ca complexes have been carried out.<sup>23</sup>

Substantial interest has been focused on 1,1-*bis*-phosphonates (or *gem-bis*-phosphonates) and *tris*-phosphonates because of their established performance as scale inhibitors in commercial applications<sup>6</sup> and the former's potential as bone growth regulators.<sup>24</sup> A review of representative literature cases of Ca-Phosphonate structures relevant to this study follows.

Uchtmann, in the early '70's described the crystal structure of a Ca-HEDP complex (HEDP = Hydroxy-Ethylidene-1,1-DiPhosphonate).<sup>22a</sup> It was found that each Ca is eight-coordinate and, in addition to two  $\text{H}_2\text{O}$  molecules, it is bound by two phosphonate oxygens and the hydroxyl group. There is an infinite array of  $\text{HEDP}^{2-}$ , water molecules and calcium ions linked together by hydrogen bonding and calcium coordination of oxygens from both  $\text{HEDP}^{2-}$  and water molecules. Intramolecular  $\text{Ca}-\text{O}(\text{PO}_3)$  distances are 2.352(4) and 2.420(3) Å, whereas the  $\text{Ca}-\text{O}(\text{H})$  bond is much longer, at 2.608(3) Å.

In addition, similar observations can be made in a similar Rb-HEDP complex. Intramolecular  $\text{Rb}-\text{O}(\text{PO}_3)$  distances are 2.949(3) and 2.952(3) Å, whereas the  $\text{Rb}-\text{O}(\text{H})$  distance is much longer, at 3.078(3) Å.<sup>25</sup> It is worth-mentioning that the  $\text{Rb}-\text{O}$  distances are much longer

than the Ca—O ones. This is because the monopositive charge on the Rb ions is less effective than the one on the Ca ions. This greatly affects the ionic nature of these bonds.

Nardelli et al. described the crystal structure of calcium dichloromethylene diphosphonate.<sup>22b</sup> The structure reveals that the phosphonate groups are monodeprotonated, and that there is extensive hydrogen bonding network. Furthermore, the Ca centers are heptacoordinate and are bonded to 5 water molecules and two phosphonate oxygens from the same chelating dichloro-methylene diphosphonate molecule. Ca—O(P) distances are 2.362(3) Å, and Ca—O(H<sub>2</sub>O) distances are in the range 2.418(4)–2.428(4) Å.

The solid-state structure and solution chemistry of the Ca salt of *N*-(phosphonomethyl)glycine (glyphosate) has been investigated by Raymond et al.<sup>20b</sup> The structure is polymeric. The Ca is seven-coordinate with four oxygen atoms from three different glyphosate groups, one carboxylate oxygen from another glyphosate and two water oxygens. Each glyphosate is in turn bonded to four different Ca atoms through both the phosphonate and carboxylate groups. The N atom is protonated and therefore does not participate in any Ca binding. One phosphonate group from the glyphosate ligand acts as a bridge between two Ca centers and brings them to a distance of 3.93 Å apart. Ca—O(P) distances vary. Ca—O(bridging) is 2.511(1) Å long, much longer than a “normal” Ca—O distance of 2.368(1) Å in the same molecule.

Mathew et al. reported the crystal structure and spectroscopic properties of a Ca complex with a novel *bis*-phosphonate, glutaryl-*bis*-phosphonate.<sup>22c</sup> This is a phosphonate that has an acyl group next to the phosphonate group. This study provides the first example of a structure of a Ca complex involving a non-geminal *bis*-phosphonate. The structure can be described in terms of a covalently pillared layer-type arrangement of neutral Ca-GlBP-Ca units along the *b*-axis. Each oxygen atom of the phosphonate group is bonded to a different Ca ion, and each Ca in turn is linked to three phosphonate groups. Ca—O(P) distances are ~2.38 Å. The Ca octahedra and the phosphonate tetrahedra form a two-dimensional polar sheet perpendicular to the *b*-axis. The chelate bonds involving the keto groups appear to be important links in the stabilization of the structure and, in turn, to the biological activity, as the authors report, of bis(acylphosphonates).

Complex formation equilibria studies of amino polyphosphonates are also found in the literature.<sup>26</sup> More specifically, Sawada et al. reported studies on Ca-AMP complex formation.<sup>27</sup> They suggested that AMP coordinates to alkaline earth metal ions in a *tetradentate* fashion (presumably at high pH's), through three phosphoryl oxygens (originating from three different PO<sub>3</sub> groups) and the central nitrogen atom. As the

pH decreases, they propose that the *tetradentate* AMP becomes *tridentate* because the central N is protonated, and gets “pushed-back,” away from the Ca center. The aforementioned proposed structure was said to be consistent with the one proposed by Nikitina et al. based on infrared vibrational measurements.<sup>28</sup>

Based on results from the present study the N atom is *indeed* protonated at pH of  $\sim 1.5$  and there is only one AMP that acts as a *bidentate* chelate. The remaining ones are *monodentate*. Direct comparison of our results with those reported by Sawada et al.<sup>27</sup> cannot be made due to the differences in pH of the two experiments. Our attempts to grow good quality crystals of Ca-AMP salts at higher pH's have thus far been unsuccessful.

### CaCO<sub>3</sub> Inhibition, Crystal Modification and Synergism Between AMP and Dispersant Polymers

The Scale Inhibition Test was used to investigate the effect of AMP as CaCO<sub>3</sub> inhibitor at high Ca<sup>2+</sup> and CO<sub>3</sub><sup>2-</sup> levels, as well as high temperatures and pH. CaCO<sub>3</sub> has increased tendency to precipitate at higher temperatures, a phenomenon known as “inverse solubility.” The experiments were run at 43°C. Bulk water temperatures in the range 40–50°C are commonly found in industrial applications.

According to the results in Table VI, AMP is an effective CaCO<sub>3</sub> scale inhibitor. It can maintain 400 ppm (of 800 ppm) of soluble calcium in solution at high supersaturation and temperature (run 1). Furthermore, its performance is assisted by the dispersant properties of polymers A and B. At Ca<sup>2+</sup>/HCO<sub>3</sub><sup>-</sup> of 800/800 CaCO<sub>3</sub> inhibition is assisted by both polymers A and B. The blend AMP/polymer A achieves 64% inhibition (run 4) and the blend AMP/polymer B is more effective with 74% inhibition (run 5). At lower supersaturations (Ca<sup>2+</sup>/HCO<sub>3</sub><sup>-</sup> of 700/700) the

**TABLE V** Scale Inhibition Test Conditions

Run	Ca (ppm)	Malk (ppm)	Mg (ppm)	AMP (ppm)	Polymer (ppm)
0	800	800	200	0	0
1	800	800	200	30	0
2	700	700	200	30	30 of A
3	700	700	200	30	30 of B
4	800	800	200	30	30 of A
5	800	800	200	30	30 of B
6	900	900	200	30	30 of A
7	900	900	200	30	30 of B



**TABLE VI** Scale Inhibition Test Results

Run	Soluble Ca (ppm), 2h	% Inhibition, 2h	Dispersed Ca (ppm), 24h	% Dispersion, 24h
0	5	<1	0	0
1	409	51	354	44
2	522	75	692	99
3	572	82	715	100
4	510	64	716	90
5	596	74	726	91
6	557	62	734	82
7	553	61	757	84

blend with polymer B performs better than the one with polymer A, 82% inhibition for the former (run 3) vs. 75% for the latter (run 2). At higher supersaturations however, ( $\text{Ca}^{2+}/\text{HCO}_3^-$  of 900/900) the performance of both blends is about the same  $\sim 60\%$  (runs 6 and 7).

The dispersant properties of polymers A and B seem to be very similar based on measurements of dispersed  $\text{Ca}^{2+}$  (Table VI). Both blends achieve quantitative dispersion of  $\text{CaCO}_3$  at  $\text{Ca}^{2+}/\text{HCO}_3^-$  levels of 700/700 (runs 2 and 3). At higher stress conditions ( $\text{Ca}^{2+}/\text{HCO}_3^-$  of 800/800) the dispersion performance is still high at  $\sim 90\%$  (runs 4 and 5), but drops to  $\sim 80\%$  at  $\text{Ca}^{2+}/\text{HCO}_3^-$  of 900/900 (runs 6 and 7).

An additional point of interest is the way AMP (together with the polymers) affects crystal and particle morphology of the resulting  $\text{CaCO}_3$  scales. In order to examine that more carefully, samples of those  $\text{CaCO}_3$  deposits were analyzed by SEM. The images are given in Figure 7.

Upon examination of the morphology of the  $\text{CaCO}_3$  scale deposits, it becomes evident that there are obvious differences.  $\text{CaCO}_3$  solids that precipitate from solutions containing AMP and polymer A (Figure 7, upper) are amorphous (non-crystalline) spheres and have little tendency to "stick" to each other. Their approximate size is  $6\ \mu$ . On the other hand,  $\text{CaCO}_3$  precipitates from AMP and polymer B solutions (Figure 7, lower) have well defined crystalline morphology, and, apparently, tend to agglomerate and form larger aggregates. The size of those particles is  $\sim 10\ \mu$ .

Dubin performed similar studies on  $\text{CaCO}_3$  crystallization in the presence of organic phosphorous compounds or polymers.<sup>29</sup> His results showed that structural variations in organophosphonate or dispersant polymer additives used in supersaturated solutions of  $\text{CaCO}_3$  caused dramatic effects on the crystal/particle morphology and size of the precipitated scale.

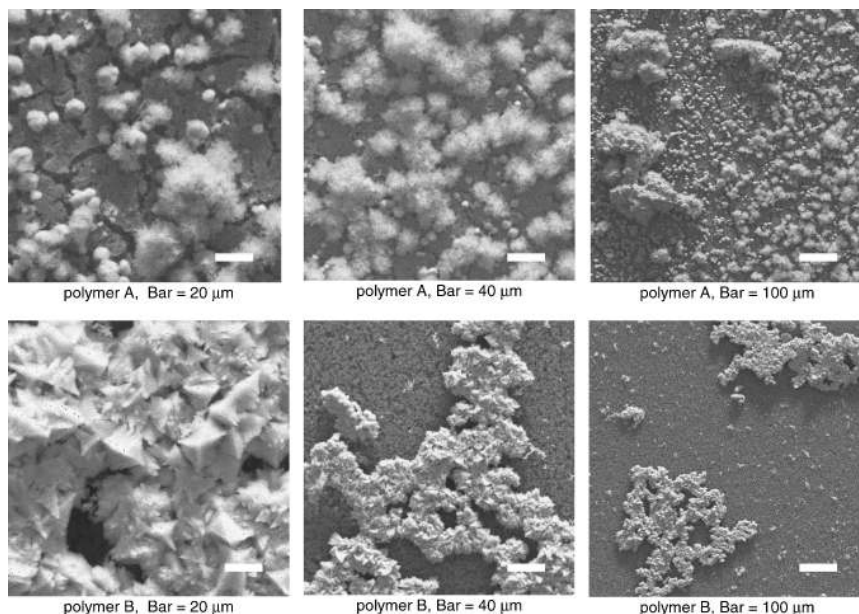


**FIGURE 7**  $\text{CaCO}_3$  precipitates from solutions containing AMP and polymers A or B as additives.

Both polymers A and B show virtually good synergistic effects with AMP in  $\text{CaCO}_3$  scale inhibition. However, polymer A causes the precipitated  $\text{CaCO}_3$  to form amorphous (and, consequently, more easily removed) scale, whereas polymer B allows the formation of larger agglomerates composed of crystalline microparticles.

The general scope of metal polyphosphonate chemistry is currently underway in our laboratory.

## CONCLUSIONS

It is obvious that the quest for the “ideal” scale inhibitor is far from over. Such an inhibitor must possess the following highly desirable properties: (a) excellent scale inhibition performance, (b) high Ca tolerance, (c) stability towards oxidizing biocides (widely used to treat microbiological growth in industrial waters),<sup>30</sup> and (d) low production cost. It is therefore crucial for researchers to investigate new chemistries along the lines defined by the above “ideal” properties.

In this paper the crystallization and structure of a Ca-AMP complex salt was described. Although the pH of its formation is different

than that usually encountered in water systems, useful projections can be made. At higher pH regimes AMP undergoes further deprotonation resulting in an increase in its effective negative charge. Therefore its complexation with  $\text{Ca}^{2+}$  will require a larger number of  $\text{Ca}^{2+}$  ions to achieve neutrality. Possible Ca-AMP precipitates include  $\text{Ca}_2(\text{AMP})$ ,  $\text{Ca}_3(\text{AMP})_2$ ,  $\text{Ca}_2(\text{AMP})$ ,  $\text{Ca}_3(\text{AMP})$ , etc. Isolation and structural characterization of such complexes are under way in our laboratory. Elegant work by Fogler et al. has focused on batch synthesis of Ca-AMP precipitates with Ca:AMP molar ratios of 1, 2, and 3 for potential applications in squeeze treatments of oil wells.<sup>9f</sup>

A better understanding of the formation of Ca-inhibitor salts may ultimately lead to effective prevention by either design and/or synthesis of inhibitors possessing specific properties or by development of appropriate dispersant polymers.<sup>31</sup> Prevention of inhibitor precipitation, coupled with control of its oxidative degradation will allow better and more economical application and control of a chemical treatment program.

## REFERENCES

- [1] a) J. C. Cowan and D. J. Weintritt, *Water-Formed Scale Deposits* (Gulf Publishing Co. Houston, TX, 1976); b) Z. Amjad (Ed.), *Mineral Scale Formation and Inhibition* (Plenum Press: New York, 1995 and references therein); c) Z. Amjad (Ed.), *Calcium Phosphates in Biological and Industrial Systems* (Kluwer Academic Publishers: Boston, 1998 and references therein); d) Z. Amjad and J. P. Hooley, *Tenside. Surf. Det.*, **31**, 12 (1994); e) Z. Amjad, *Can. J. Chem.*, **66**, 2180 (1988); f) J. E. Oddo and M. B. Tomson, *SPE Production & Facilities*, **February**, 47 (1994).
- [2] a) F. N. Kemmer, *The Nalco Water Handbook* (McGraw-Hill Company, New York, 1988); b) *Betz handbook of industrial water conditioning* (Betz Laboratories, Inc., B Trevose, Pennsylvania 1980).
- [3] a) J. N. Tanis, *Procedures of Industrial Water Treatment* (Ltan Inc., Ridgefield, CT: 1987); b) J. Katzel, *Plant Engineering*, **27**, 32 (1989); c) Power Special Report, *Power*, **March**, S-1 (1973); d) E. C. Elliot, *Power*, **December**, S-1 (1985); e) C. R. Branan, *Rules of Thumb for Chemical Engineers* (Gulf Publishing Co. Houston, TX, 1994), p. 127; f) K. D. Demadis, *Chemical Processing*, **May**, 29 (2003).
- [4] a) W. W. Frenier, *Technology for Chemical Cleaning of Industrial Equipment* (NACE Press: Houston, TX, 2001, and references therein); b) J. W. McCoy, *Industrial Chemical Cleaning* (Chemical Publishing: New York, 1984).
- [5] a) G. Poff, *Mater. Perform.*, **10**, 24 (1978); b) C. Wohlberg and J. R. Buchholz, *Corrosion/75*, Paper No. 143 (National Association of Corrosion Engineers, Houston, TX, 1975); c) C. W. Smith, *Industrial Water Treatment*, **July/August**, 20 (1993); d) W. S. Midkiff and H. P. Foyt, *Materials Performance*, **August**, 39 (1979); e) W. S. Midkiff and H. P. Foyt, *Materials Performance*, **February**, 17 (1978); f) W. S. Midkiff and H. P. Foyt, Cooling Technology Institute, TP77-16 (TP-169A); g) W. S. Midkiff and H. P. Foyt, Los Alamos Scientific Laboratory, Report LA-UR-76-660 (1976); h) W. S. Midkiff, Los Alamos Scientific Laboratory, Report LA-5508-MS (March 1974).
- [6] a) Dequest: Phosphonates by Solutia (Introductory Guide), Publication # 7459151B; b) Dequest: Phosphonates by Solutia (2054 Phosphonates for scale and corrosion

- control, chelation, dispersion), Publication # 7450006A; c) Dequest: Phosphonates by Solutia (2060-S, 2066 & 2066-A Phosphonates: metal ion control agents), Publication # 7459369; d) Dequest: Phosphonates by Solutia (2000 & 2006 Phosphonates for scale and corrosion control, chelation, dispersion), Publication # 7459023B.
- [7] a) J. Gill and R. G. Varsanik, *J. Cryst. Growth*, **76**, 57 (1986); b) J. M. Matty and M. B. Tomson, *Appl. Geochem.*, **3**, 549 (1988); c) M. B. Tomson, *J. Cryst. Growth*, **62**, 106 (1983); d) H. Blum and P. Christophliemk, *Phosphorus Sulfur Silicon*, **30**, 619 (1987); e) Z. Amjad, *J. Colloid Interface Sci.*, **123**, 523 (1988).
  - [8] a) W. F. Masler and Z. Amjad, *Corrosion/88*, Paper No. 11 (National Association of Corrosion Engineers, Houston, TX, 1988); b) V. Deluchat, J.-C. Bollinger, B. Serpaud, and C. Caullet, *Talanta*, **44**, 897 (1997); d) J. E. Oddo and M. B. Tomson, *Applied Geochem.*, **5**, 527 (1990).
  - [9] a) F. M. Sweeney and S. D. Cooper, *Society of Petroleum Engineers International Symposium on Oilfield Chemistry, New Orleans, LA March 2-5*, paper SPE 25159 (1993); b) J. E. Oddo and M. B. Tomson, *Corrosion/92*, Paper No. 34 (National Association of Corrosion Engineers, Houston, TX, 1992); c) J. Xiao, A. T. Kan, and M. B. Tomson, *American Chemical Society-Division of Fuel Chemistry, Symposium Preprints*, **43**, 246 (1998); d) F. H. Browning and H. S. Fogler, *AIChE Journal*, **42**, 2883 (1996); e) O. J. Vetter, *J. Pet. Tech.*, **March**, 339 (1973); f) R. Pairat, C. Sumeath, F. H. Browning, and H. S. Fogler, *Langmuir*, **13**, 1791 (1997); h) F. H. Browning and H. S. Fogler, *AIChE Journal*, **42**, 2883 (1996).
  - [10] a) R. P. Carter, R. L. Carrol, and R. R. Irani, *Inorg. Chem.*, **6**, 939 (1967); b) D. Hasson, R. Semiat, D. Bramson, M. Busch, and B. Limoni-Relis, *Desalination*, **118**, 285 (1998); c) J. S. B. Gill, *Desalination*, **124**, 43 (1999); d) O. A. Hamed, M. A. K. Al-Sofi, M. Imam, K.B. Mardouf, A. S. Al-Mobayed, and A. B. Ehsan, *Desalination*, **128**, 275 (2000); e) J. S. Gill, *International Water Conference*, **paper # 23**, 93 (1995).
  - [11] a) V. S. Sastri, *Corrosion inhibitors: principles and applications* (Chichester, New York: Wiley, 1998); b) C. C. Nathan, (Ed.), *Corrosion Inhibitors* (NACE International: Houston, TX, 1973); c) Y. I. Kuznetsov, *Organic inhibitors of corrosion of metals* (Plenum Press: New York, 1996); d) European Federation of Corrosion, *Corrosion Inhibitors* (Publication # 11, The Institute of Metals: London, England, 1994); e) I. H. Farooqi, M. A. Nasir, and M. Quraishi, *Corr. Prev. & Control*, **October**, 129 (1997).
  - [12] a) M. M. Reddy and G. H. Nancollas, *Desalination*, **12**, 61 (1973); b) M. B. Tomson, *J. Cryst. Growth*, **62**, 106 (1983); c) P. G. Klepetsanis and P. G. Koutsoukos, *J. Cryst. Growth*, **193**, 156 (1998); d) N. G. Harmandas, E. Navarro Fernandez, and P. G. Koutsoukos, *Langmuir*, **14**, 1250 (1998); e) M. Dalpi, E. Karayianni, and P. G. Koutsoukos, *J. Chem. Soc. Faraday Trans.*, **89**, 965 (1993); f) A. G. Xyla, J. Mikroyannidis, and P. G. Koutsoukos, *J. Colloid Interface Sci.*, **153**, 537 (1992).
  - [13] a) Z. Amjad, *Tenside Surf. Det.*, **34**, 102 (1997); b) W. F. Masler, III and Z. Amjad, European Patent Application 0 267 597 A2; c) E. B. Smyk, J. E. Hoots, K. P. Fivizzani, and K. E. Fulks, *Corrosion/88*, Paper No. 14 (National Association of Corrosion Engineers, Houston, TX, 1988); d) J. E. Hoots and G. A. Crucil, *Corrosion/86*, Paper No. 13 (National Association of Corrosion Engineers, Houston, TX, 1986); e) L. W. Becker, European Patent Application 0 109 200 A1, (1984).
  - [14] a) R. W. Kaesler and D. W. Fong. US patent 4,983,686 (1991); b) D. W. Fong. US patent 4,795,789 (1989); c) J. E. Hoots, D. A. Johnson, and D. W. Fong. US patent 4,756,881 (1988); d) D. J. Kowalski and D. W. Fong. US patent 4,490,308, (1985); e) D. W. Fong and B. Vallino, Jr. European Patent Application EP 265846 (1988); f) D. W. Fong. German Patent DE 3616583 (1987).

- [15] C. K. Johnson, *ORTEP: A fortran thermal ellipsoid plot program* (Technical Report ORNL-5138, Oak Ridge National Laboratory: Oak Ridge, TN, 1976).
- [16] E. J. Gabe, Y. Le Page, J.-P. Charland, F. L. Lee, and P. S. White, *J. Appl. Crystallogr.*, **22**, 384 (1989).
- [17] *International Tables for X-ray Crystallography* (Kynoch Press: Birmigham, U.K., 1974), vol. IV.
- [18] Spectral assignments were made based on information from the following references: a) L. J. Bellamy, *The Infrared Spectra of Complex Molecules* (Chapman and Hall, London: 1975); b) N. L. Alpert, W. E. Keiser, and H. A. Szymanski, *IR: Theory and Practice of Infrared Spectroscopy*, (2nd ed., Plenum Press: New York, 1970); c) G. Socrates, *Infrared Characteristic Group Frequencies: Tables and Charts* (2nd ed., Wiley: Chichester, U.K., 1994); d) L. C. Thomas, *Interpretation of the Infrared Spectra of Organophosphorous Compounds* (Heyden: London, 1974).
- [19] a) A. H. Reis, Jr., S. W. Peterson, M. E. Dryan, E. Gebert, G. W. Mason, and D. F. Peppard, *Inorg. Chem.*, **15**, 2748 (1976); b) M. E. Dryan, A. H. Reis, Jr., E. Gebert, S. W. Peterson, G. W. Mason, and D. F. Peppard, *J. Am. Chem. Soc.*, **98**, 4801 (1976).
- [20] a) G. Cao, V. M. Lynch, J. S. Swinnea, and T. E. Mallouk, *Inorg. Chem.*, **29**, 2112 (1990); b) P. H. Smith and K. N. Raymond, *Inorg. Chem.*, **27**, 1056 (1988); c) D. Gibson and R. Karaman, *J. Chem. Soc. Dalton Trans.*, 1911, (1989); d) K. J. Langley, P. J. Squattrito, F. Adani, and E. Montoneri, *Inorg. Chim. Acta*, **253**, 77 (1996); e) G. Cao, H. Lee, V. M. Lynch, and T. E. Mallouk, *Solid State Ionics*, **26**, 63 (1988).
- [21] a) R.-M. Schloth, E. Lork, F. U. Seifert, G.-V. Rösenthaller, H. Cohen, G. Golomb, and E. Breuer, *Naturwissenschaften*, **83**, 571 (1996); b) D. DeLaMatter, J. J. McCullough, and C. Calvo, *J. Phys. Chem.*, **77**, 1146 (1973); c) S. W. Peterson, E. Gebert, A. H. Reis, Jr., M. E. Dryan, G. W. Mason, and D. F. Peppard, *J. Phys. Chem.*, **81**, 466 (1977); d) E. Gebert, A. H. Reis, Jr., M. E. Dryan, S. W. Peterson, G. W. Mason, and D. F. Peppard, *J. Phys. Chem.*, **81**, 471 (1977); e) V. S. Sergienko, E. O. Tolkacheva, and A. B. Ilyukhin, *Zh. Neorg. Khim.*, **38**, 1129 (1993); f) L. M. Shkol'nikova, E. G. Afonin, E. V. Kalugina, and S. S. Sotman, *Kristallografiya*, **36**, 77 (1991); g) R. Rochdaoui, J. P. Silvestre, Q. D. Nguyen, M. R. Lee, and A. Neuman, *Acta Crystallog. Sect. C Cryst. Struct. Comm.*, **C46**, 2083 (1990); h) J. P. Silvestre, N. El Messbahi, R. Rochdaoui, Q. D. Nguyen, M. R. Lee, and A. Neuman, *Acta Crystallog. Sect. C Cryst. Struct. Comm.*, **C46**, 986 (1990); i) E. G. Afonin, N. I. Pechurova, O. P. Gladkikh, A. A. Masyuk, and L. M. Shkol'nikova, *Zh. Obshch. Khim.*, **58**, 2646 (1988); j) B. L. Barnett and L. C. Strickland, *Acta Crystallog. Sect. B*, **B35**, 1212 (1979); k) V. A. Uchtman and R. A. Gloss, *J. Phys. Chem.*, **76**, 1298 (1972).
- [22] a) V. A. Uchtman, *J. Phys. Chem.*, **76**, 1304 (1972); b) M. Nardelli, G. Pelizzi, G. Staibano, and E. Zucchi, *Inorg. Chim. Acta*, **80**, 259 (1983); c) M. Mathew, B. O. Fowler, E. Breuer, G. Golomb, I. S. Alferiev, and N. Eidelman, *Inorg. Chem.*, **37**, 6485 (1998).
- [23] a) J.-P. Björkroth, M. Peräkylä, T. A. Pakkanen, and E. Pohjala, *J. Comput.-Aided Mol. Des.*, **6**, 303 (1992); b) M. Peräkylä, T. A. Pakkanen, J.-P. Björkroth, and E. Pohjala, *J. Chem. Soc. Perkin Trans.*, **2**, 1167 (1992); c) J. P. Räsänen, M. Peräkylä, E. Pohjala, and T. A. Pakkanen, *J. Chem. Soc. Perkin Trans.*, **2**, 1055 (1994); d) J. P. Räsänen, E. Pohjala, and T. A. Pakkanen, *J. Chem. Soc. Perkin Trans.*, **2**, 2485 (1994); e) J. P. Räsänen, E. Pohjala, and T. A. Pakkanen, *J. Chem. Soc. Perkin Trans.*, **2**, 39 (1995); f) J. P. Räsänen, E. Pohjala, H. Nikander, and T. A. Pakkanen, *J. Phys. Chem.*, **100**, 8230 (1996); g) J. P. Räsänen, E. Pohjala, H. Nikander, and T. A. Pakkanen, *J. Phys. Chem. A*, **101**, 5196 (1997).
- [24] a) O. L. M. Bijvoet, H. A. Fleisch, R. E. Canfield, and R. G. G. Russell, (Eds.), *Bisphosphonates on Bone* (Elsevier Science: Basel 1995); b) B. Y. Klein,

- H. Ben-Bassat, E. Breuer, V. Solomon, and G. Golomb, *J. Cell. Biochem.*, **68**, 186 (1998); c) G. Golomb, J. M. Van Gelder, I. S. Alferiev, A. Ornoy, A. Hoffman, A. Schlossman, A. Friedman-Ezra, N. El-Hanany-Rozen, and R. Chen, *Phosphorus, Sulfur Silicon Relat. Elem.*, **221**, 109–110, (1996).
- [25] P. P. Charpin, M. Lance, M. Nierlich, D. Vigner, M.-R. Lee, J.-P. Silvestre, and N. Q. Dao, *Acta Crystallog. Sect. C Cryst. Struct. Comm.*, **C44**, 990 (1988).
- [26] a) D. Vanderpool, *International Water Conference*, **paper # 40**, 383 (1997); b) S. Westerback, K. S. Rajan, A. E. Martell, *J. Am. Chem. Soc.*, **87**, 2567 (1965); c) R. J. Motekaitis, I. Murase, and A. E. Martell, *Inorg. Nucl. Chem. Lett.*, **7**, 1103 (1971); d) R. J. Motekaitis, I. Murase, A. E. Martell, *Inorg. Chem.*, **15**, 2303 (1976); e) M. T. Zaki, E. N. Rizkalla, *Talanta*, **27**, 423 (1980); f) E. N. Rizkalla, and M. T. Zaki, *Talanta*, **26**, 507 (1979); g) E. N. Rizkalla and M. T. Zaki, *Talanta*, **27**, 769 (1980); h) K. Moedrizier, R. R. Irani, *J. Org. Chem.*, **31**, 1603 (1966); i) R. P. Carter, R. L. Carrol, and R. R. Irani, *Inorg. Chem.*, **6**, 939 (1967); j) B. H. Wiers, *Inorg. Chem.*, **10**, 2581 (1971); k) T. Fonong, D. J. Burton, and D. J. Pietrzyk, *Anal. Chem.*, **55**, 1089 (1983).
- [27] K. Sawada, T. Araki, and T. Suzuki, *Inorg. Chem.*, **26**, 1199 (1987).
- [28] a) M. I. Kabachnik, T. Y. Medved, N. M. Dyatlova, and M. V. Rudomino, *Russ. Chem. Rev.*, **43**, 733 (1974); b) L. V. Nikitina, A. I. Grigor'ev, and N. M. Dyatlova, *Zh. Obsch. Khim.*, **44**, 1669 (1974).
- [29] L. Dubin, Corrosion/80, Paper No. 222 (National Association of Corrosion Engineers, Houston, TX, 1980).
- [30] a) R. D. Bartholomew, *International Water Conference*, **paper # 74**, 523 (1998). b) M. Vaska, and W. Go, *Industrial Water Treatment*, **March/April**, 39 (1993).
- [31] K. D. Demadis, in *Compact Heat Exchangers and Enhancement Technology for the Process Industries*, R. K. Shah, Editor (Begell House Inc., 2003), p. 483.

## APPENDIX

Note added in proof. While this paper was in press we discovered two relevant papers to AMP. (1) Synthesis and Structure of  $\text{Na}_2[(\text{HO}_3\text{PCH}_2)_3\text{NH}]\cdot 1.5\text{H}_2\text{O}$ : The First Alkaline Triphosphonate, *J. Solid State Chem.*, **151**, 122 (2000) by H. Silvia Martínez-Tapia, Aurolio Cabeza, Sebastián Bruque, Pilar Perticra, Santiago García-Granda and Miguel A. G. Aranda and (2) Nitrilotris(methylenephosphonates) in aqueous solution and solid state—dilatometric, potentiometric and NMR investigations, *Inorg. Chim. Acta*, **357**, 797 (2004) by Gisbert Grossmann, Kim A. Burkov, Gerhard Hägele, Lubov A. Myund, Stephan Hermens, Claudia Verwey and Sholban M. Arat-ool.